Robust Non-Minimum-Phase Compensation for a Class of Uncertain Dynamical Systems

Kuk-Whan Byun* and Bong Wie†
Arizona State University, Tempe, Arizona 85287
and
John Sunkel‡
NASA Johnson Space Center, Houston, Texas 77058

This paper presents robust control synthesis techniques for uncertain dynamical systems subject to structured parameter perturbation. Both classical and H_∞ control synthesis techniques are investigated. Most H_∞-related control techniques are not directly concerned with the structured parameter perturbation. In this paper, however, a new way of incorporating the parameter uncertainty in the robust H_∞ control design is explored. A generic model of uncertain dynamical systems is used to illustrate the design methodologies developed in this paper. It is shown that, for a certain class of noncollocated structural control problems, use of either technique results in non-minimum-phase compensation.

I. Introduction

A NEW concept of generalized structural filtering (GSF) and its application to active vibration control synthesis are presented in Ref. 1. The GSF concept emphasizes the use of non-minimum-phase compensation, which has zeros in the right-half s plane. It is shown in Ref. 1 that, for a certain class of noncollocated structural control problems, non-minimum-phase compensation provides the proper phase lag to increase the closed-loop damping of the flexible modes while maintaining good performance and robustness to pole/zero uncertainty. Application of a "robustified" linear quadratic Gaussian (LGQ) technique to a noncollocated structural control problem has also resulted in such a non-minimum-phase compensator.[2] However, non-minimum-phase compensators have rarely been used by practicing control designers. Non-minimum-phase compensation is also avoided by control researchers since there exists a lower bound on possible maximum sensitivity of a feedback control system with non-minimum-phase zeros.[3] In general, arbitrarily small sensitivity over certain frequency regions necessitates a large sensitivity at other frequencies. Since the sensitivity function should satisfy a certain integral constraint over all frequency ranges,[3] it is not practical to design a control system with arbitrarily small sensitivity over a wide frequency range. Hence, mixed sensitivity minimization[4,5] is desirable, which may result in non-minimum-phase compensation.

In this paper, both frequency-domain and state-space techniques are investigated for robust control synthesis. A generic model of uncertain dynamical systems is used as an example to illustrate the design concepts and methodologies. Horowitz's quantitative feedback theory (QFT)[6-8] is examined, in particular for a dynamical system with uncertain poles near the imaginary axis. The merits of non-minimum-phase compensation, despite its well-known disadvantage, become apparent when the QFT approach is properly employed. A robust control synthesis technique based on H_∞ control theory is also developed in this paper, incorporating structured real-parameter variations in state-space formulation[9-11] of robust H_∞ control design. In this approach, system matrices possessing uncertain parameters are linearly decomposed into an internal feedback loop.

In conventional H_∞ control techniques,[12] the plant uncertainty is included in a weighting matrix as a ball function that surrounds the plant uncertainty. Consequently, a parameter variation is not explicitly considered in conventional H_∞ control synthesis techniques. The LGQ/LTR (loop transfer recovery) approach deals basically with unstructured uncertainties, often resulting in cancellations of the plant dynamics by the compensator. Whenever these cancellations occur near the imaginary axis, the closed-loop system becomes very sensitive to the plant pole/zero uncertainty. Also, a stability robustness measure based on singular value is generally too conservative. In order to cope with structured uncertainties, a structured singular value concept based on block-structured, complex-parameter variations is developed in Ref. 13. A stability robustness measure based on this concept becomes also too conservative for real-parameter variations. A modified LQG/LTR approach proposed in Ref. 14 utilizes the input-output decomposition concept of Ref. 15 to incorporate parameter variations. A robust H_∞ control synthesis technique to be presented in this paper exploits such a parameter uncertainty modeling concept. For the design example of this paper, use of this technique also results in non-minimum-phase compensation.

This paper is organized as follows. A classical control design methodology is discussed in Sec. II, where the QFT approach to robust single-input single-output (SISO) control synthesis is examined with emphasis on the usefulness of the GSF concept in shaping a proper loop transfer function. Section III presents a new, robust control synthesis technique that incorporates structured parameter perturbations in H_∞ control synthesis. Whereas the frequency-domain method discussed in Sec. II is primarily restricted to SISO systems, the state-space method developed in Sec. III is applicable to multivariable control systems. In Sec. IV, a generic example of uncertain dynamical

Received Aug. 10, 1989; presented as Paper 89-3516 at the AIAA Guidance, Control, and Navigation Conference, Boston, MA, Aug. 14-16, 1989; revision received Jan. 22, 1991; accepted for publication Feb. 12, 1991.

*Postdoctoral Fellow; currently, Research Scientist, Dynacs Engineering Company, 34650 U.S. Highway 19N, Suite 301, Palm Harbor, FL 34684. Member AIAA.

†Associate Professor, Department of Mechanical and Aerospace Engineering. Associate Fellow AIAA.

‡Aerospace Engineer, Mail Code EG2. Member AIAA.

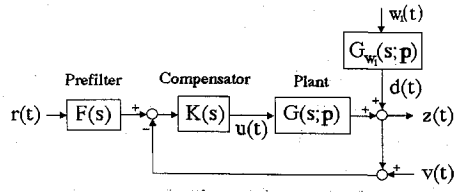

Fig. 1 Block diagram representation of a feedback control system.

systems is formulated, and both classical and robust H_∞ control designs are performed for this example.

II. Robust Frequency-Domain Control Synthesis

In this section, we consider SISO control system analysis and design based on classical frequency-domain concepts to provide the foundation for robust compensator design using the QFT and GSF concepts.

Figure 1 shows a block diagram representation of a feedback control system with the following transfer function relations:

$$z(s) = G(s;p)u(s) + d(s) \tag{1}$$

$$u(s) = K(s)\left[F(s)r(s) - z(s) - v(s)\right] \tag{2}$$

The plant transfer function $G(s;p)$ contains a constant but uncertain parameter vector p. It is assumed that the parameter uncertainty is bounded as $\underline{p} < p < \bar{p}$, where $\underline{p}$ and $\bar{p}$ are the lower and upper bounds of the uncertain parameter vector, respectively. The reference input and the control input are denoted as $r(t)$ and $u(t)$, respectively. The equivalent output disturbance $d(t)$ is modeled as the output from $G_{w_1}(s;p)$ driven by the plant disturbance $w_1(t)$, where $G_{w_1}(s;p)$ is in general different from $G(s;p)$. The system output $z(t)$ is fed back to the compensator $K(s)$ with the sensor noise $v(t)$ added.

The compensator $K(s)$ is to be designed to meet various control requirements. The prefilter $F(s)$ can be used for deliberate shaping of the reference input $r(s)$. In this paper, however, prefiltering of the reference input is not considered, hence, $F(s) = 1$.

Sensitivity Analysis

The tracking error response $e(s) = r(s) - z(s)$ is related to the external inputs $r(s)$, $d(s)$, and $v(s)$ by

$$e(s) = S(s;p)\left[r(s) - d(s)\right] + T(s;p)v(s) \tag{3}$$

where

$$S(s;p) \triangleq \left[1 + L(s;p)\right]^{-1} \tag{4}$$

$$T(s;p) \triangleq L(s;p)\left[1 + L(s;p)\right]^{-1} \tag{5}$$

$$L(s;p) \triangleq G(s;p)K(s) \tag{6}$$

and $S(s;p)$ is the sensitivity function, $T(s;p)$ the complementary sensitivity function, and $L(s;p)$ the loop transfer function. Since $T(s;p) + S(s;p) = 1$, a design tradeoff between the sensitivity and complementary sensitivity functions is necessary.

The control input $u(s)$ is related to the external inputs $r(s)$, $d(s)$, and $v(s)$ by

$$u(s) = Q(s;p)\left[r(s) - d(s) - v(s)\right] \tag{7}$$

where

$$Q(s;p) \triangleq K(s)\left[1 + L(s;p)\right]^{-1} \tag{8}$$

which should be proper in order not to saturate the control input. As a result, it is desired that the compensator $K(s)$ have more poles than zeros.

Nominal transfer functions are defined for the nominal plant parameter p_0 as

$$G_0(s) \triangleq G(s;p_0) \tag{9}$$

$$L_0(s) \triangleq G(s;p_0)K(s) \tag{10}$$

$$S_0(s) \triangleq S(s;p_0) \tag{11}$$

$$T_0(s) \triangleq T(s;p_0) \tag{12}$$

$$Q_0(s) \triangleq Q(s;p_0) \tag{13}$$

Changes in L, S, T, and Q caused by the plant perturbation $\Delta G(s) \triangleq G(s;p) - G_0(s)$ can be obtained as

$$\Delta L(s) = \Delta G(s)K(s) \tag{14}$$

$$\Delta S(s) = -S(s;p)\Delta L(s)S_0(s) \tag{15}$$

$$\Delta T(s) = S(s;p)\Delta L(s)S_0(s) \tag{16}$$

$$\Delta Q(s) = -K(s)S(s;p)\Delta L(s)S_0(s) \tag{17}$$

Variations in L, S, T, and Q are directly related to the tracking error and control input saturation and must be kept small with respect to parameter perturbation. The closed-loop sensitivity with respect to the loop transfer function uncertainty can be reduced simply by minimizing a suitable norm of the sensitivity function, for example, the infinity norm of weighted sensitivity.

Stability/Performance Specifications

An important issue in characterizing the stability margin of a feedback system is to properly determine the upper bounds on S, T, and Q. If the plant uncertainty is modeled in the frequency domain, proper shaping of the loop transfer function is possible using a Nichols chart. Generalization of this SISO stability robustness problem to multi-input/multi-output (MIMO) cases is also possible using the return difference S^{-1} and the inverse return difference T^{-1} (Ref. 16).

The bounds on $|T(j\omega)|$ for a minimum phase system are often specified as

$$a(\omega) \le |T(j\omega)| \le b(\omega) \tag{18}$$

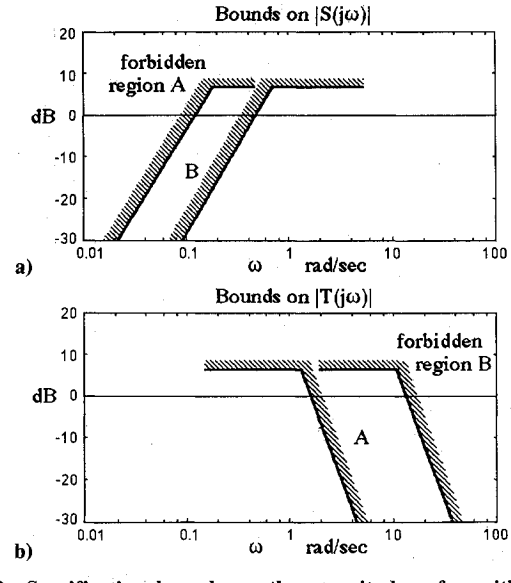

Fig. 2 Specification bounds on the magnitudes of sensitivity and complementary sensitivity functions: a) bounds on $|S(j\omega)|$; b) bounds on $|T(j(\omega)|$.

where $a(\omega)$ and $b(\omega)$ are the lower and upper bounds of $|T(j\omega)|$, respectively. Specifications for a non-minimum-phase system should include phase restrictions since the magnitude alone does not completely specify the time response of such a system.[17] The sensor noise reduction specification is often transformed into bounds on the bandwidth and cutoff rate of $|T(j\omega)|$ in the high-frequency region. Also, tracking performance specification is transformed to bounds on the cutoff frequency and slope of $|S(j\omega)|$ in the low-frequency region. When both sensor noise reduction and good tracking performance are required, bounds on $S(j\omega)$ can be used for the low-frequency range, bounds of $T(j\omega)$ for the high-frequency range, and bounds on either $|S(j\omega)|$ or $|T(j\omega)|$ for middle frequency ranges. Figures 2 illustrate such mixed sensitivity bound specifications.

Nichols Chart and Inverse Nichols Chart

The bounds on $|S(j\omega)|$ and $|T(j\omega)|$ are related to the bounds on the loop transfer function $L(j\omega)$. A quantitative relation among these functions is readily available in polar plots or Nichols charts. If a plant uncertainty model is to be incorporated in control system design, it is more convenient to use a Nichols chart than a polar plot since the shape of the plant uncertainty at a specific frequency in a Nichols chart is not affected by the feedback compensation.

Command-response and sensor noise-response analyses are usually performed using a Nichols chart since constant magnitude and phase loci of the closed-loop transfer function $T(j\omega)$ are related to the loop transfer function $L(j\omega) = G(j\omega)K(j\omega)$ by

$$T(j\omega) = L(j\omega)/\left[1+L(j\omega)\right] \tag{19}$$

While tracking-response analysis of plant disturbance can be performed in the conventional Nichols chart, more accurate sensitivity anslysis can be done in the low-frequency region by using the so-called inverse Nichols chart. The sensitivity function is related to the inverse loop transfer function by

$$S(j\omega) = 1/\left[1+L(j\omega)\right] = L^{-1}(j\omega)/\left[1+L^{-1}(j\omega)\right] \tag{20}$$

Disturbance-response or sensitivity analysis is then performed by 1) using $L^{-1}(j\omega)$ in the conventional Nichols chart, or 2) using the inverse Nichols chart, where the constant magnitude/phase loci of $T(j\omega)$ are rotated by 180 deg. The second approach is preferred since two specifications on $|S(j\omega)|$ and $|T(j\omega)|$ in different frequency ranges can be overlayed to form mixed sensitivity bounds for loop transfer function shaping.

Quantitative Feedback Theory/Generalized Structural Filtering Synthesis

Horowitz's quantitative feedback theory is essentially a graphical design method that utilizes the classical frequency-domain concepts discussed previously. In particular, the method exploits the Nichols chart with constant closed-loop magnitude and phase loci and the so-called parameter uncertainty templates. The method incorporates the concept of designing a robust control system that guarantees the desired performance over a prescribed region of plant parameter uncertainty.

At each frequency ω, perturbation in the plant maps to the set of complex numbers

$$\Delta G(\omega) = \left\{G(j\omega;\boldsymbol{p}), \underline{p} < p < \bar{p}\right\} \tag{21}$$

The values of $G(j\omega;\boldsymbol{p})$ over the range of plant parameters are calculated, and the boundary shape is referred to as a $\Delta G(\omega)$ template. Calculation of $\Delta G(\omega)$ templates is a non-trivial problem, especially for a system with uncertain poles and zeros near the imaginary axis.

At each selected frequency, the $\Delta G(\omega)$ template is manipulated to determine the bound on the nominal loop transfer function $L_0(j\omega)$, denoted as $B(\omega)$, using the specified $|T(j\omega)|$ or $|S(j\omega)|$ bounds. If a nominal loop transfer function at ω is inside the forbidden $B(\omega)$ bound, the performance specification is violated at that frequency. Proper shaping of $L_0(j\omega)$ to avoid the $B(\omega)$ bound at each frequency guarantees the desired performance and stability over a prescribed region of plant parameter uncertainty.

However, proper shaping of the nominal loop transfer function for a system with many uncertain poles and zeros near the imaginary axis is not a trivial task. In such a case, the GSF concept of Ref. 1 may be useful since the concept exploits the use of non-minimum-phase compensation, which allows various combinations of gain and phase.

A robust control design procedure based on the QFT and GSF concepts can be summarized as the following.

1) Given uncertain parameter ranges and bounds on $|T(j\omega)|$ or $|S(j\omega)|$, select some frequencies that properly describe the plant uncertainty $\Delta G(\omega)$.

2) At each selected frequency, determine the values of $G(j\omega;\boldsymbol{p})$ over the range of plant parameters and draw the associated $\Delta G(\omega)$ template on the Nichols chart.

3) At each selected frequency, manipulate the $\Delta G(\omega)$ template to determine the bound on $L_0(j\omega)$, the so-called $B(w)$ bound, using the specified $|T(j\omega)|$ or $|S(j\omega)|$ bounds.

4) Shape the desired $L_0(j\omega)$ and synthesize a compensator $K(s)$ by using various combinations of generalized second-order filters developed in Ref. 1. While a computer-aided or optimization-based procedure for this step can be employed, proper shaping of the nominal loop transfer function often requires the designer's intuition and experience.

In summary, application of the frequency-domain method discussed in this section is primarily restricted to SISO control system design. It is basically a graphical design method based on trial-and-error iterations and the designer's physical intuition and experience, which is considered by control theoreticians as the most significant shortcoming of classical frequency-domain methods. In the next section, we develop a state-space approach to robust control problems that may overcome some drawbacks of classical frequency-domain techniques.

III. Robust H_∞ Control Synthesis

In recent years, there has been a growing interest in robust stabilization and control based on H_∞ control theory.[12,18-21] Substantial contributions have also been made to the state-space characterization of the H_∞ control problems.[9,10] In this section, a robust H_∞ control synthesis technique is developed for uncertain dynamical systems with structured parameter variations. Although most H_∞-related control techniques are not directly concerned with the structured parameter uncertainty, a new way of incorporating the parameter uncertainty in robust H_∞ control design is presented in this section.

The H_∞ space consists of functions that are bounded and stable. The H_∞ norm of a real-rational matrix $T(s)$ is defined as

$$\|T\|_\infty \triangleq \sup\left\{\|T(s)\|: \mathrm{Re}(s)>0\right\}$$

$$= \sup_\omega \|T(j\omega)\|$$

where $\|T(j\omega)\|$ is defined as the largest singular value of $T(j\omega)$ for a given ω. The state-space characterization of H_∞ control theory is employed here to develop a robust H_∞ control synthesis technique.

Consider a linear, time-invariant MIMO system described by

$$\dot{x}(t) = Ax(t) + B_1 w(t) + B_2 u(t) \tag{22a}$$

$$z(t) = C_1 x(t) + D_{11} w(t) + D_{12} u(t) \tag{22b}$$

$$y(t) = C_2 x(t) + D_{21} w(t) + D_{22} u(t) \tag{22c}$$

where $x(t)$ is an n-dimensional state vector, $w(t)$ an m_1-dimensional disburbance vector, $u(t)$ an m_2-dimensional control vector, $z(t)$ a p_1-dimensional controlled output vector, and $y(t)$ a p_2-dimensional measurement vector.

The transfer function representation of this system is given by

$$\begin{bmatrix} z(s) \\ y(s) \end{bmatrix} = \begin{bmatrix} P_{11}(s) & P_{12}(s) \\ P_{21}(s) & P_{22}(s) \end{bmatrix} \begin{bmatrix} w(s) \\ u(s) \end{bmatrix} \tag{23}$$

whereas the plant transfer matrix $P(s)$ is related to the matrices in Eqs. (22) by

$$P(s) = \begin{bmatrix} C_1 \\ C_2 \end{bmatrix} (sI - A)^{-1} [B_1 B_2] + \begin{bmatrix} D_{11} & D_{12} \\ D_{21} & D_{22} \end{bmatrix} \tag{24}$$

Internal Feedback Loop

In order to utilize the concept of an internal feedback loop, an uncertain dynamical system is described as

$$\begin{bmatrix} \dot{x} \\ z \\ y \end{bmatrix} = \begin{bmatrix} \hat{A} & \hat{B}_1 & \hat{B}_2 \\ C_1 & D_{11} & D_{12} \\ \hat{C}_2 & \hat{D}_{21} & \hat{D}_{22} \end{bmatrix} \begin{bmatrix} x \\ w \\ u \end{bmatrix} \tag{25}$$

where C_1, D_{11}, and D_{12} are not subject to parameter variations. The perturbed system matrix in Eq. (25) can be linearly decomposed as follows:

$$\begin{bmatrix} \dot{x} \\ z \\ y \end{bmatrix} = \left\{ \begin{bmatrix} A & B_1 & B_2 \\ C_1 & D_{11} & D_{12} \\ C_2 & D_{21} & D_{22} \end{bmatrix} + \Delta_p \right\} \begin{bmatrix} x \\ w \\ u \end{bmatrix} \tag{26}$$

where the first matrix on the right side is the nominal system matrix and Δ_p is the perturbation matrix defined as

$$\Delta_p \triangleq \begin{bmatrix} \Delta A & \Delta B_1 & \Delta B_2 \\ 0 & 0 & 0 \\ \Delta C_2 & \Delta D_{21} & \Delta D_{22} \end{bmatrix} \tag{27}$$

Suppose that there are l independent parameters $p_1, \ldots, p_l$ and that they are bounded as $\underline{p}_i \le p_i \le \bar{p}_i$ or $|\Delta p_i| \le 1$. The perturbation matrix Δ_p is then decomposed with respect to each parameter variation as

$$\Delta_p = -\sum_{i=1}^{l} \Delta p_i \begin{bmatrix} \alpha_x^{(i)} \\ 0 \\ \alpha_y^{(i)} \end{bmatrix} \begin{bmatrix} \beta_x^{(i)} & \beta_w^{(i)} & \beta_u^{(i)} \end{bmatrix} \tag{28}$$

where the matrices

$$\begin{bmatrix} \alpha_x^{(i)} \\ 0 \\ \alpha_y^{(i)} \end{bmatrix} \quad \text{and} \quad \begin{bmatrix} \beta_x^{(i)} & \beta_w^{(i)} & \beta_u^{(i)} \end{bmatrix}$$

span, respectively, the columns and the rows of Δ_p with respect to p_i and a rank-one dependency is assumed. Equation (28) can be rewritten in matrix form as

$$\Delta_p = -\begin{bmatrix} M_x \\ 0 \\ M_y \end{bmatrix} E \begin{bmatrix} N_x & N_w & N_u \end{bmatrix} = -MEN \tag{29}$$

where

$$M_x = \left[\alpha_x^{(1)}, \ldots, \alpha_x^{(l)}\right], \qquad M_y = \left[\alpha_y^{(1)}, \ldots, \alpha_y^{(l)}\right] \tag{30}$$

$$N_x = \begin{bmatrix} \beta_x^{(1)} \\ \vdots \\ \beta_x^{(l)} \end{bmatrix}, \quad N_w = \begin{bmatrix} \beta_w^{(1)} \\ \vdots \\ \beta_w^{(l)} \end{bmatrix}, \quad N_u = \begin{bmatrix} \beta_u^{(1)} \\ \vdots \\ \beta_u^{(l)} \end{bmatrix} \tag{31}$$

$$E = \begin{bmatrix} \Delta p_1 & & 0 \\ & \ddots & \\ 0 & & \Delta p_l \end{bmatrix} \tag{32}$$

This form of input-output decomposition of the system matrix perturbation is an extension of the work by Morton and McAfoos,[15] which has been applied to a μ test for a real-parameter variation problem. In recent years, there has been a growing interest in this kind of parameter uncertainty modeling for robust control design.

By introducing the following new variables

$$z_p \triangleq \begin{bmatrix} N_x & 0 & N_w & N_u \end{bmatrix} \begin{bmatrix} x \\ w_p \\ w \\ u \end{bmatrix} \tag{33a}$$

$$w_p \triangleq -Ez_p \tag{33b}$$

the perturbed system, Eq. (26), and the input-output decomposition, Eq. (29), can be combined as

$$\begin{bmatrix} \dot{x} \\ z_p \\ z \\ y \end{bmatrix} = \begin{bmatrix} A & M_x & B_1 & B_2 \\ N_x & 0 & N_w & N_u \\ C_1 & 0 & D_{11} & D_{12} \\ C_2 & M_y & D_{21} & D_{22} \end{bmatrix} \begin{bmatrix} x \\ w_p \\ w \\ u \end{bmatrix} \tag{34a}$$

$$w_p = -Ez_p \tag{34b}$$

where w_p and z_p are considered as the fictitious input and output, respectively, due to the plant perturbation; E is considered a fictitious, internal feedback loop gain matrix.

The internal feedback loop representation, given by Eqs. (34), becomes useful for the stability/performance robustness analysis to be discussed later in this section. This representation is also introduced in Refs. 13 and 14 for robust control synthesis with structured plant uncertainty. Bryson et al.[2] proposes the use of modal equations and fictitious disturbances acting on uncertain modes, resulting in a model for parameter uncertainty, which is similar to that of the input-output decomposition approach. If the matrix E is nonlinear in the uncertain parameters, a linearization can be employed as done in Ref. 11.

Stability/Performance Robustness

The parameter uncertainty model given by Eq. (29) and the nominal plant described by Eq. (23) can be combined as

$$\begin{bmatrix} z_p \\ z \\ y \end{bmatrix} = \begin{bmatrix} G_{11} & G_{12} & G_{13} \\ G_{21} & G_{22} & G_{23} \\ G_{31} & G_{32} & G_{33} \end{bmatrix} \begin{bmatrix} w_p \\ w \\ u \end{bmatrix} \tag{35a}$$

$$w_p = -Ez_p \tag{35b}$$

$$u = -Ky \tag{35c}$$

where w_p and z_p are the fictitious input and output, respectively, E is the fictitious internal loop gain matrix, and $K(s)$ a feedback compensator to be designed.

After closing the control loop with a stabilizing controller $K(s)$, we get the following representation of the closed-loop system:

$$\begin{bmatrix} z_p \\ z \end{bmatrix} = T \begin{bmatrix} w_p \\ w \end{bmatrix} \tag{36a}$$

$$w_p = -Ez_p \tag{36b}$$

where

$$T = \begin{bmatrix} T_{11} & T_{12} \\ T_{21} & T_{22} \end{bmatrix} \tag{37a}$$

$$T_{11} = G_{11} - G_{13}K(I + G_{33}K)^{-1}G_{31} \tag{37b}$$

$$T_{12} = G_{12} - G_{13}K(I + G_{33}K)^{-1}G_{32} \tag{37c}$$

$$T_{21} = G_{21} - G_{23}K(I + G_{33}K)^{-1}G_{31} \tag{37d}$$

$$T_{22} = G_{22} - G_{23}K(I + G_{33}K)^{-1}G_{32} \tag{37e}$$

The actual closed-loop transfer matrix from w to z under plant perturbations is then obtained as

$$T_{zw} = T_{22} - T_{21}E(I + T_{11}E)^{-1}T_{12} \tag{38}$$

Note that, in Eqs. (35) and (36), the parameter uncertainty does not appear in the transfer matrices. Equations (36) can be used for the stability/performance robustness characterization. Assuming convex parameter variations and using the small gain theorem,[12] sufficient conditions for robust stability and performance are provided by the following Theorems 1 and 2.

Theorem 1 (stability robustness). $T_{zw}(s,\alpha E)\forall\alpha \in [0,1]$ is robustly stable for $\|E\| \le \epsilon$, and $\epsilon > 0$, if

$$\|T_{11}(s)\|_\infty < \epsilon^{-1}$$

where ϵ is a design specification on the parameter variation E in Eq. (32).

Proof. This theorem can be proved by ensuring that the closed-loop characteristic polynomial remains nonsingular at all frequencies; that is,

$$\det[I + T_{11}(j\omega)E] \neq 0 \qquad \forall\omega \tag{39}$$

Detailed proof can be found in Refs. 11, 14, and 19. ■

It is seen that T_{11} determines the stability robustness with respect to parameter uncertainty. Small $\|T_{11}\|_\infty$ allows large parameter variations for closed-loop stability. However, this theorem provides a sufficient condition for closed-loop stability, resulting in a conservative control design.

For a nonconservative control design, weighted parameter variations or μ synthesis may be desirable in handling structured parameter variations. For simplicity, however, the conservative condition represented by this theorem is employed in this paper for developing a robust H_∞ control synthesis technique. Since the condition in Theorem 1 is concerned with a deterministic bound, H_∞ control theory is employed for the internal feedback loop model. The next theorem provides a sufficient condition for guaranteed performance robustness.

Theorem 2 (performance robustness). $T_{zw}(s,\alpha E)\forall\alpha \in [0,1]$ is stable, and $\|T_{zw}(s,\alpha E)\|_\infty < \gamma \forall\alpha \in [0,1]$ with $\|E\| \le \gamma^{-1}$, if

$$\|T\|_\infty < \gamma \tag{40}$$

where T and T_{zw} are defined in Eqs. (36) and (38), and γ is an upper bound for the desired performance specification.

Proof. Proof of this theorem can be found in Ref. 11.

These two theorems provide conditions for robust stability and performance of the perturbed closed-loop system in terms of T_{11} and T in Eqs. (36). The following theorem gives a robust H_∞ controller that satisfies the condition in Eq. (40). The following redefinition of z, w, and the associated matrices enables us to employ the standard state-space representation given by Eqs. (22):

$$z \leftarrow \begin{bmatrix} z_p \\ z \end{bmatrix}, \qquad w \leftarrow \begin{bmatrix} w_p \\ w \end{bmatrix}$$

$$B_1 \leftarrow [M_x \quad B_1], \qquad C_1 \leftarrow \begin{bmatrix} N_x \\ C_1 \end{bmatrix}$$

$$D_{11} \leftarrow \begin{bmatrix} 0 & N_w \\ 0 & D_{11} \end{bmatrix}, \qquad D_{12} \leftarrow \begin{bmatrix} N_u \\ D_{12} \end{bmatrix}$$

$$D_{21} \leftarrow [M_y \quad D_{21}] \tag{41}$$

Theorem 3 (H_∞-suboptimal controller). Assume that

1) (A,B_2) is stabilizable and (C_2,A) is detectable.

2) $D_{12}^T[C_1 \quad D_{12}] = [0 \quad I]$.

3) $\begin{bmatrix} B_1 \\ D_{21} \end{bmatrix} D_{21}^T = \begin{bmatrix} 0 \\ I \end{bmatrix}$.

4) The rank of $p_{12}(j\omega)$ and $p_{21}(j\omega)$ is m_2 and p_2, respectively, for all ω.

5) $D_{11} = 0$ and $D_{22} = 0$.

Given assumptions 1-5, there exists an internally stabilizing controller such that, for the closed-loop transfer matrix T in Eqs. (36) and for a given design variable γ,

$$\|T\|_\infty < \gamma$$

if and only if the following Riccati equations

$$0 = A^TX + XA - X\left(B_2B_2^T - \frac{1}{\gamma^2}B_1B_1^T\right)X + C_1^TC_1 \tag{42}$$

$$0 = AY + YA^T - Y\left(C_2^TC_2 - \frac{1}{\gamma^2}C_1^TC_1\right)Y + B_1B_1^T \tag{43}$$

have unique symmetric positive semidefinite solutions X and Y such that 1) $A - (B_2B_2^T - 1/\gamma^2 B_1B_1^T)X$ is stable, 2) $A - Y(C_2^TC_2 - 1/\gamma^2 C_1^TC_1)$ is stable, and 3) $(I - 1/\gamma^2 YX)^{-1}Y$ is positive semidefinite.

An H_∞-suboptimal controller that satisfies $\|T_{zw}\|_\infty < \gamma$, where γ is a design variable specifying an upper bound of the perturbed closed-loop performance T_{zw}, is then obtained as

$$K(s) = K\left[sI - A - \frac{1}{\gamma^2}B_1B_1^TX + B_2K + LC_2\right]^{-1}L \tag{44}$$

where

$$K = B_2^TX \tag{45}$$

$$L = \left(I - \frac{1}{\gamma^2}YX\right)^{-1}YC_2^T \tag{46}$$

Proof. This theorem is only valid for the case with $D_{11} = 0$ and $D_{22} = 0$. Detailed proof can be found in Refs. 9-11 and 20. ■

IV. Design Examples

In order to highlight the concepts and methodologies presented in the previous sections, a generic model of uncertain dynamical systems used in Refs. 1 and 2 is employed here as an example of a system with a single uncertain parameter. It will be shown that for this example use of either technique results in non-minimum-phase compensation. Although there are some drawbacks of such unconventional compensation, the concept of robust, non-minimum-phase compensation has been experimentally validated by closed-loop tests of the Mini-

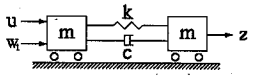

Fig. 3 A lightly damped two-mass-spring system.

Mast truss structure.[22] Further refinement of this example problem with three uncertain parameters can be found in Refs. 23 and 24. An application of the proposed robust H_∞ control synthesis technique to a more realistic spacecraft control problem is presented in Ref. 25; however, a simple two-mass-spring example is used here to illustrate the design methodologies developed in this paper.

Consider a two-mass-spring-damper system with noncollocated actuator and sensor, shown in Fig. 3. The transfer function description is given by

$$y(s) = \frac{cs+k}{ms^2(ms^2+2cs+2k)}\,u(s) \tag{47}$$

where $m=1$, $c=0.002$, $0.5<k<2.0$ with nominal spring constant $k_0=1$, which corresponds to a nominal damping ratio of $\zeta_0=0.0014$. This system can be represented in state-space form as

$$\begin{bmatrix}\dot{x}_1\\ \dot{x}_2\\ \dot{x}_3\\ \dot{x}_4\end{bmatrix} = \begin{bmatrix}0 & 1 & 0 & 0\\ -k & -c & k & c\\ 0 & 0 & 0 & 1\\ k & c & -k & -c\end{bmatrix}\begin{bmatrix}x_1\\ x_2\\ x_3\\ x_4\end{bmatrix} + \begin{bmatrix}0\\ 1\\ 0\\ 0\end{bmatrix}u + \begin{bmatrix}0\\ 1\\ 0\\ 0\end{bmatrix}w_1 \tag{48a}$$

$$z = \begin{bmatrix}x_3\\ u\end{bmatrix} \tag{48b}$$

$$y = x_3 + v \tag{48c}$$

where w_1 and v are plant disturbance and sensor noise, respectively. The problem is to design a compensator that stabilizes the system over $0.5<k<2.0$. First, the QFT/GSF approach is used to design a robust compensator for this problem. The robust H_∞ control synthesis technique presented in Sec. III is then employed for the same problem.

Frequency-Domain Control Design

The plant uncertainty associated with the variation in the spring constant is first examined. Perturbation in the plant maps to the set

$$\Delta G(\omega) = \left\{\frac{0.002j\omega+k}{(j\omega)^2\left[(j\omega)^2+0.004j\omega+2k\right]};\quad 0.5<k<2.0\right\}$$

Since the plant has only one uncertain parameter k, it is easy to form the bounds $B(\omega)$ on $L_0(j\omega)$ for closed-loop stability. The $B(\omega)$ bounds on $L_0(j\omega)$ for closed-loop stability are obtained by tracing the loci of the nominal points of $\Delta G(\omega)$ templates as these templates are translated around the $(-180$-deg, 0-dB) point. Since the plant has no right-half-plane poles, the Nyquist stability criterion implies that $L(j\omega;k)$ with $0.5<k<2.0$ must be shaped so as not to encircle the point $(-180$ deg, 0 dB) in the Nichols chart. The nominal curve $L_0(j\omega)$ is likewise shaped so as not to encircle this point and additionally to avoid the $B(\omega)$ bounds. The performance bounds on $|S(j\omega)|$ and $|T(j\omega)|$ in Fig. 2 can also be incorporated using constant magnitude loci in the Nichols chart.

Figure 4, for example, shows $B(\omega)$ bounds for stability robustness. The $B(\omega)$ bounds for performance robustness have similar patterns. Although the $B(\omega)$ bounds for stability robustness are represented as closed curves in the Nichols chart, $L_0(j\omega)$ must be shaped well away from these bounds. The nominal loop transfer function $L_0(j\omega)$ has a high peak at $\omega=1.414$ rad/s due to the lightly damped, oscillatory mode at that frequency. However, the $B(1.414)$ bound is located within $0\text{ dB}<|B(1.414)|<50$ dB and $-300\text{ deg}<\angle B(1.414)<-60$ deg. Hence, $L_0(j1.414)$ must be located to avoid the range $-60\text{ deg}<\angle B(1.414)<60$ deg. This large phase change required for $L_0(j\omega)$ can be accomplished by either phase-lead or phase-lag compensation. The GSF concept[1] was found to be very useful in shaping the nominal loop transfer function since the concept provides various combinations of generalized second-order filters, including non-minimum-phase filters.

The following non-minimum-phase compensator can be found to yield a $L_0(j\omega)$, which satisfies the given $B(\omega)$ bounds:

$$K(s) = 0.086\,\frac{\left[(s/0.15)+1\right]\left[(s/2)^2-2(0.5)(s/2)+1\right]}{\left[(s/1.60)+1\right]\left[(s/2)^2+2(0.5)(s/2)+1\right]} \tag{49}$$

Figure 5 shows a root locus plot vs overall loop gain in which each point corresponds to a 0.2 increment in gain. The nominal closed-loop poles are denoted by a square, and the nominal closed-loop system has a 6-dB gain margin.

A different non-minimum-phase compensator, which is basically a high-pass filter satisfying an additional performance specification (given by Fig. 2), has been designed by Yaniv and Horowitz and is included here for comparison:

$$K(s) = 0.5\,\frac{\left[(s/0.7)^2-2(0.1)(s/0.7)+1\right]}{\left[(s/2)^2+2(0.3)(s/2)+1\right]} \times \frac{(s/0.5+1)(s/1.5+1)(s/2.5+1)}{\left[(s/22)^2+2(0.5)(s/22)+1\right]^2}$$

A root locus vs overall loop gain of this compensator is shown in Fig. 6, and the nominal closed-loop system has a gain margin >6 dB. Although this compensator is non-minimum-phase, its overall characteristic is similar to that of a high-pass, phase-lead, minimum-phase compensation discussed in Ref. 1. That is, this compensator has a large loop-gain increase at high frequencies, similar to minimum-phase compensators in Refs. 26 and 27.

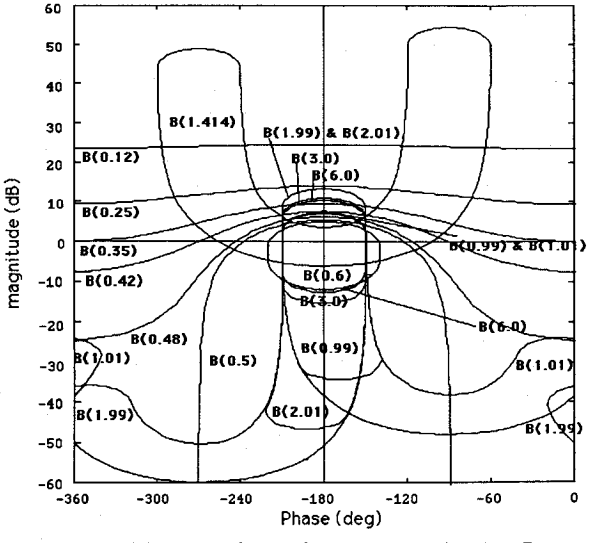

Fig. 4 $B(\omega)$ bounds for performance specification B.

Robust H_∞ Control Design

For the state-space description of the same example with the uncertain parameter k, described by Eq. (48a), the variation ΔA is decomposed as

$$\Delta A = -\Delta k \begin{bmatrix} 0 \\ 1 \\ 0 \\ -1 \end{bmatrix} \begin{bmatrix} 1 & 0 & -1 & 0 \end{bmatrix} \tag{50}$$

Note that ΔA is spanned by the matrices

$$M = \begin{bmatrix} 0 \\ 1 \\ 0 \\ -1 \end{bmatrix}, \qquad N = \begin{bmatrix} 1 & 0 & -1 & 0 \end{bmatrix}$$

where M is the fictitious disturbance distribution matrix spanning the columns of ΔA, and N is the fictitious controlled output distribution matrix spanning the rows of ΔA. The fictitious input and output for this example are expressed as

$$z_p = Nx = x_1 - x_3, \qquad w_p = -\Delta k z_p \tag{51}$$

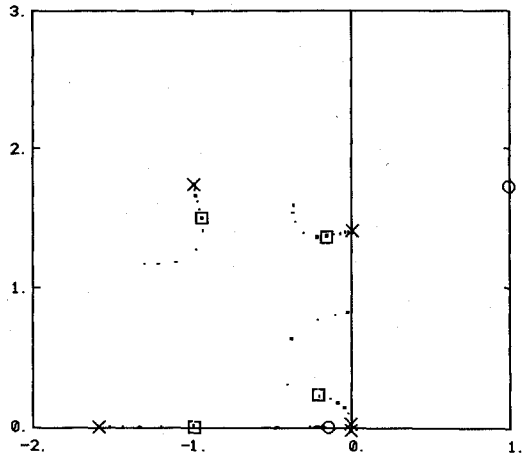

Fig. 5 Root locus vs overall loop gain for a compensator with a non-minimum-phase, all-pass structural filter with a 6-dB gain margin.

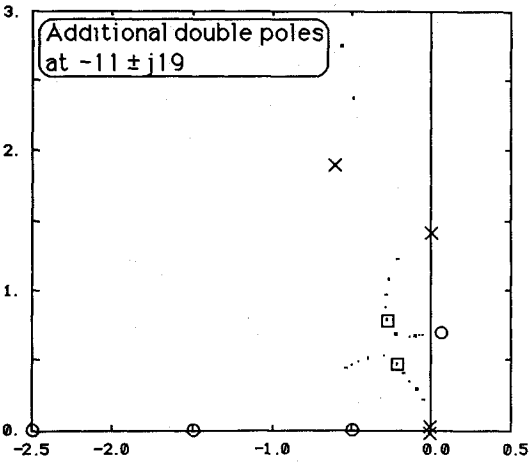

Fig. 6 Root locus vs overall loop gain for a non-minimum-phase, high-pass compensator with a gain margin >6 dB.

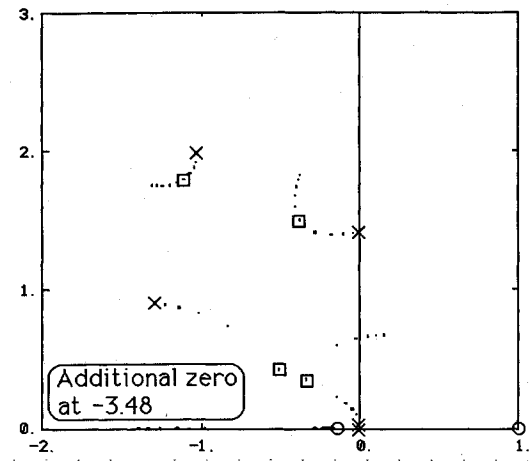

Fig. 7 Root locus vs overall loop gain for a robust H_∞ compensator with a 3.28-dB gain margin.

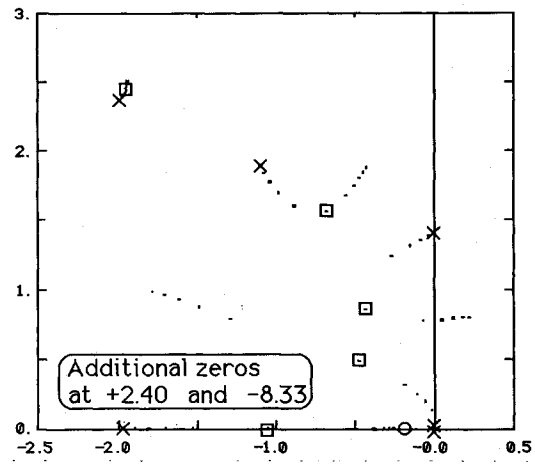

Fig. 8 Root locus vs overall loop gain for a robustified LQG compensator with a 2.5-dB gain margin.

Equations (51) replace the parameter variation in Eqs. (48) as follows:

$$\begin{bmatrix} \dot{x}_1 \\ \dot{x}_2 \\ \dot{x}_3 \\ \dot{x}_4 \end{bmatrix} = \begin{bmatrix} 0 & 1 & 0 & 0 \\ -k_0 & -c & k_0 & c \\ 0 & 0 & 0 & 1 \\ k_0 & c & -k_0 & -c \end{bmatrix} \begin{bmatrix} x_1 \\ x_2 \\ x_3 \\ x_4 \end{bmatrix} + \begin{bmatrix} 0 \\ 1 \\ 0 \\ 0 \end{bmatrix} u + \begin{bmatrix} 0 \\ 1 \\ 0 \\ 0 \end{bmatrix} w_1 + \begin{bmatrix} 0 \\ 1 \\ 0 \\ -1 \end{bmatrix} w_p \tag{52a}$$

$$\begin{bmatrix} z_p \\ z \end{bmatrix} = \begin{bmatrix} x_1 - x_3 \\ x_3 \\ u \end{bmatrix} \tag{52b}$$

$$y = x_3 + v \tag{52c}$$

where w_1 and v are the plant disturbance and sensor noise, respectively.

This input-output decomposition has an interesting physical interpretation when the system is represented in modal coordinates. The fictitious disturbance w_p is acting on the flexible

mode, and the fictitious controlled output z_p is to be added to the robust control of the uncertain flexible mode $(x_1 - x_3)$. In robust LQG design by Bryson et al.,[2] the flexible modal coordinate $(x_1 - x_3)$ is selected for output weighting and a fictitious disturbance is acting on the flexible mode.

By defining

$$w \leftarrow \begin{bmatrix} w_p \\ w_1 \\ v \end{bmatrix}, \qquad z \leftarrow \begin{bmatrix} z_p \\ z \end{bmatrix} \tag{53}$$

the system matrices in Eqs. (22) with definitions in Eq. (41) can be represented as

$$A = \begin{bmatrix} 0 & 1 & 0 & 0 \\ -k_0 & -c & k_0 & c \\ 0 & 0 & 0 & 1 \\ k_0 & c & -k_0 & -c \end{bmatrix}$$

$$B_1 = \begin{bmatrix} 0 & 0 & 0 \\ 1 & 1 & 0 \\ 0 & 0 & 0 \\ -1 & 0 & 0 \end{bmatrix}, \qquad B_2 = \begin{bmatrix} 0 \\ 1 \\ 0 \\ 0 \end{bmatrix}$$

$$C_1 = \begin{bmatrix} 1 & 0 & -1 & 0 \\ 0 & 0 & 1 & 0 \\ 0 & 0 & 0 & 0 \end{bmatrix}, \qquad D_{12} = \begin{bmatrix} 0 \\ 0 \\ 1 \end{bmatrix}$$

$$C_2 = \begin{bmatrix} 0 & 0 & 1 & 0 \end{bmatrix}, \qquad D_{21} = \begin{bmatrix} 0 & 0 & 1 \end{bmatrix}$$

and $D_{11} = 0$, $D_{22} = 0$.

To achieve the desired closed-loop performance over all frequencies, T_{zw} often includes frequency-dependent weighting matrices. A proper selection of the weighting matrices is an important step in any optimization-based design techniques, such as LQG and H_∞ optimization. For the example design considered here, the disturbances w_p, w_1, and v are multiplied by weighting factors, 0.1, 0.025, and 0.025, respectively. The performance specification bound γ is chosen to be 1. The weighting factors and γ represent relative disturbance levels and overall closed-loop performance level, respectively. Note that a proper selection of the weighting factors and γ to meet the desired performance/robustness requires trial-and-error iterations and the designer's physical intuition and experience.

By solving two Riccati equations, Eqs. (42) and (43), the following robust H_∞ compensator, which satisfies stability robustness over the prescribed region of the plant parameter uncertainty $(0.5 \le k \le 2.0)$ and also satisfies the scaled performance, can be found as

$$K(s) = \frac{0.083[(s/0.15)+1][-(s/0.99)/+1]}{[(s/1.58)^2 + 2(0.82)(s/1.58)+1]} \times \frac{[(s/3.48)+1)]}{[(s/2.24)^2 + 2(0.46)(s/2.24)+1]} \tag{54}$$

Figure 7 shows a root locus vs overall loop gain of this compensator; the gain margin is 3.28 dB. This robust H_∞ compensator has a non-minimum-phase real zero, which is comparable to a robustified LQG design by Bryson et al.[8]:

$$K(s) = \frac{0.15[(s/0.20)+1][-(s/2.40)+1]}{[(s/1.96)+1][(s/2.19)^2 + 2(0.49)(s/2.19)+1]} \times \frac{[(s/8.33)+1]}{[(s/3.11)^2 + 2(0.65)(s/3.11)+1]} \tag{55}$$

A root locus plot vs overall loop gain of this compensator is also shown in Fig. 8. This LQG controller, robustified with respect to the uncertain spring stiffness k, has a 2.5-dB gain margin.

Remarks

Some comments on the merits and drawbacks of non-minimum-phase compensation are made here. In particular, an issue regarding the relatively small gain margins of the robust H_∞ and robustified LQG controllers is briefly discussed here.

For the example problem of this paper, it is possible to design a minimum-phase compensation with a large gain margin (e.g., see Refs. 26 and 27). However, such a high-pass, phase-lead, minimum-phase controller inevitably results in a large loop-gain increase at high frequencies, and it would amplify any measurement noise intolerably. Furthermore, it may destabilize any unmodeled high-frequency flexible modes. On the other hand, most non-minimum-phase compensation results in significant rolloffs at the expense of small gain margins at lower frequencies. Consequently, a relatively small gain margin is often inevitable for a properly designed, non-minimum-phase compensator with a large parameter robustness margin. It is, however, possible to improve the gain margin of a non-minimum-phase compensator by considering the loop gain as one of uncertain parameters, as discussed in Ref. 24.

Much more work is needed, however, to further explore some tradeoffs among gain/phase margins, parameter margin, and high-frequency rolloff. Some detailed discussions on this issue can be found in Refs. 1 and 24.

V. Conclusions

Robust control synthesis techniques for uncertain dynamical systems subject to structured parameter perturbations have been presented. For the simple example considered in the paper, use of either the classical or modern H_∞-based technique has resulted in non-minimum-phase compensation. Much more work is needed, however, to further explore the merits and drawbacks of non-minimum-phase compensation.

Acknowledgments

This research was supported in part by NASA Langley Research Center under the Control Structure Interaction Guest Investigator Program and by NASA Johnson Space Center under Grant NAG9-279. The authors gratefully acknowledge the constructive comments of Bernard Friedland for improving the quality of this paper.

References

[1]Wie, B., and Byun, K. W., "New Generalized Structural Filtering Concept for Active Vibration Control Synthesis," *Journal of Guidance, Control, and Dynamics,* Vol. 12, No. 2, 1989, pp. 147-154.

[2]Bryson, A. E., Jr., Hermelin, S., and Sun, J., "LQG Controller Design for Robustness," American Control Conference, Seattle, WA, June 1986.

[3]Freudenburg, J. S., "Sensitivity Reduction, Nonminimum Phase Zeros and Design Tradeoffs in Single Loop Feedback Systems," *Proceedings of the IEEE Control and Decision Conference,* 1983.

[4]Kwakernaak, H., "Minimax Frequency Domain Performance and Robustness Optimization of Linear Feedback Systems," *IEEE Transactions on Automatic Control,* Vol. AC-30, No. 10, 1985.

[5]Verma, M., and Jonckheere, E., "L^∞-Compensation with Mixed

Sensitivity as a Broadband Matching Problem," *Systems & Control Letters,* Vol. 4, 1984.

[6]Horowitz, I. M., "Quantitative Feedback Theory," *IEE Proceedings,* Pt. D, Vol. 129, Nov. 1982.

[7]Horowitz, I. M., and Sidi, M., "Synthesis of Feedback Systems with Large Plant Ignorance for Prescribed Time-Domain Tolerances," *International Journal of Control,* Vol. 16, Feb. 1972.

[8]Yaniv, O., and Horowitz, I. M., "A Quantitative Design Method for MIMO Linear Feedback Systems Having Uncertain Plants," *International Journal of Control,* Vol. 43, No. 2, 1986, pp. 401–421.

[9]Doyle, J., Glover, K., Khargonekar, P., and Francis, B., "State-Space Solutions to Standard H_2 and H_∞ Control Problems," *IEEE Transactions on Automatic Control,* Vol. 34, No. 8, 1989, pp. 831–847.

[10]Glover, K., and Doyle, J., "State-Space Formulae for All Stabilizing Controllers that Satisfy an H_∞-Norm Bound and Relations to Risk Sensitivity," *Systems & Control Letters,* No. 11, 1988, pp. 167–172.

[11]Byun, K.-W., "Robust Controller Synthesis for Uncertain Dynamical Systems," Ph.D. Dissertation, Dept. of Aerospace Engineering, University of Texas at Austin, Austin, TX, Dec. 1989.

[12]Francis, B. A., *A Course in H_∞ Control Theory,* Springer-Verlag, Berlin, Germany, 1987.

[13]Doyle, J., "Analysis of Feedback Systems with Structured Uncertainties," *IEE Proceedings,* Pt. D, Vol. 129, No. 6, 1982.

[14]Tahk, M., and Speyer, J. L., "Modeling of Parameter Variations and Asymptotic LQG Synthesis," *IEEE Transactions on Automatic Control,* Vol. AC-32, No. 9, 1987, pp. 793–801.

[15]Morton, B. G., and McAfoos, R. M., "A Mu-Test for Robustness Analysis of a Real-Parameter Variation Problem," *Proceedings of American Control Conference,* June 1985, pp. 135–138.

[16]Safonov, M. G., Laub, A. J., and Hartmann, G. L., "Feedback Properties of Multivariable Systems: The Role and Use of the Return Difference Matrix," *IEEE Transactions on Automatic Control,* Vol. AC-26, No. 1, 1981, pp. 47–65.

[17]Horowitz, I. M., and Liao, Y.-K., "Limitations of Non-Minimum Phase Feedback Systems," *International Journal of Control,* Vol. 40, No. 5, 1984, pp. 1003–1013.

[18]Zames, G., "Feedback and Optimal Sensitivity: Model Reference Transformations, Multiplicative Seminorms, and Approximate Inverses," *IEEE Transactions on Automatic Control,* Vol. AC-26, No. 2, 1981, pp. 301–320.

[19]Kimura, H., "Robust Stability for a Class of Transfer Functions," *IEEE Transactions on Automatic Control,* Vol. AC-29, No. 9, 1984, pp. 788–793.

[20]Kimura, H., "Conjugation, Interpolation, Model-Matching in H^∞," *International Journal of Control,* Vol. 49, No. 1, 1989, pp. 269–307.

[21]Ball, J. A., and Cohen, N., "Sensitivity Minimization in an H^∞ Norm: Parametrization of All Suboptimal Solutions," *International Journal of Control,* Vol. 46, No. 3, 1987, pp. 785–816.

[22]Wie, B., Horta, L., and Sulla, J., "Classical Control System Design and Experiment for the Mini-Mast Truss Structure," *Journal of Guidance, Control, and Dynamics,* Vol. 14, No. 4, 1991, pp. 778–784.

[23]Wedell, E., Chuang, C.-H., and Wie, B., "Computational Analysis of a Stability Robustness Margin for Structured Real-Parameter Perturbations," *Journal of Guidance, Control, and Dynamics,* Vol. 14, No. 3, 1991, pp. 607–614.

[24]Wie, B., Liu, Q., and Byun, K.-W., "Robust H_∞ Control Synthesis Method and Its Application to a Benchmark Problem," *Journal of Guidance, Control, and Dynamics* (to be published).

[25]Byun, K.-W., Wie, B., Geller, D., and Sunkel, J., "Robust H_∞ Control Design for the Space Station with Structured Parameter Uncertainty," *Journal of Guidance, Control, and Dynamics* (to be published).

[26]Franklin, G. F., and Powell, J. D., *Feedback Control of Dynamic Systems,* Addison-Wesley, Reading, MA, 1986, pp. 450–473.

[27]Chiang, R. Y., and Safonov, M. G., "H_∞ Robust Control Synthesis for an Undamped, Noncolocated Spring-Mass System," *Proceedings of the 1990 American Control Conference,* May 1990, pp. 966–967.